Discover Materials

Review

In-situ microscopy and digital image correlation to study the mechanical characteristics of polymer-based materials

Seyedtaghi Mousavi[1] · **John G. Hardy**[2,3]

Received: 24 September 2024 / Accepted: 3 February 2025
Published online: 18 February 2025

Abstract
In-situ microscopic methods can help researchers to analyse microstructural changes of materials structures under different conditions (e.g., temperature and pressure) at various length scales. Digital Image Correlation (DIC) combines image registration and tracking to enable accurate measurements of changes in materials in 2D and 3D. This review focuses on combining microscopy and DIC to study the properties of materials (including natural/synthetic biomaterials, biological samples and their composites) in academic, public and industry settings, including exciting examples of bioimaging.

Article highlights

- In-situ microscopic methods facilitate understanding of microstructural changes of materials.
- The DIC technique can be used with optical and non-optical microscopic methods.
- The DIC technique is applicable for a broad range of length scales and time scales.
- The techniques are applicable for a variety of soft and hard materials and their composites, including natural/biological materials.

Keywords Composites · Digital image correlation · In-situ optical microscopy · In-situ non-optical microscopy · Materials characterization

1 Introduction

Polymer composites are ubiquitous in our everyday lives because of their functional/mechanical properties [1], the mechanical properties of such materials are underpinned by the nanoscale/microscale features constituting the structures [2], and there are some excellent reviews on this topic [3–7]. Traditional mechanical testing methods obtain information about the macroscopic physical properties of polymers and their composites, and it is important to note that that can miss information about the contribution of the nanoscale/microscale structures present in these materials [8], and there is significant interest in applying such methods to analyzing biological samples (particularly to assess cell mechanics) [9]. Correlation of multi-scale structures and macroscopic properties is an area of current analytical research [10, 11]; a variety of different laboratory and computational techniques can be employed to understand

✉ Seyedtaghi Mousavi, tghmousavi90@gmail.com; ✉ John G. Hardy, j.g.hardy@lancaster.ac.uk | [1]Department of Biochemistry, Payame Noor University, P. O. Box 19395-3697, Tehran, Iran. [2]Department of Chemistry, Lancaster University, Lancaster, Lancashire LA1 4YB, UK. [3]Materials Science Lancaster, Lancaster University, Lancaster, Lancashire LA1 4YB, UK.

the behavior of polymers and their composites [12–15]. Methods for mechanical characterization (e.g., compressive, tensile, rheology, etc.) at various length scales coupled with DIC have been employed to analyze polymer-based materials (including composites) undergoing large deformations [16–18]; e.g., polylactide-based materials [19], the thermoset elastomer polyurea [20], shape-memory polymers [21], 3D printed polymeric metamaterials [22], all cellulose composites [23], nitrile rubber composites [24], fiber reinforced polypropylene composites [25], glass fiber reinforced thermoplastics [26], carbon black-silicone composites [27], polymer fiber reinforced concrete [28].

The DIC technique (Fig. 1) [29] is one of the most frequently exploited methods used with optical and non-optical microscopic methods (e.g., atomic force microscopy [AFM], scanning electron microscopy [SEM], etc.) for measurements from the nm to cm scale, potentially employing both 2D DIC (with a single camera) and 3D DIC or stereo DIC (with 2 synchronized cameras) to achieve high-spatial-resolution imaging [16, 17, 30]. The fundamental DIC procedure involves application of a speckle pattern to a surface, capturing a series of digital images during mechanical testing, followed by DIC analysis to determine displacements/strains on the surface [30–32].

A significant challenge in all DIC applications (including local DIC and global DIC [GDIC]) involves creating optimized DIC patterns for specimens via preparation of speckle patterns on test sample surfaces [16, 17, 30–34]; the macroscale DIC patterns are mostly random grey scale patterns that are deposited via a variety of techniques [30, 34, 35]; for nanoscale patterning drop casting or spraying droplets of nanoparticle-loaded solvents are popular, however, the homogeneity of particle density is a challenge because they tend to cluster [35–39]. In correlative imaging samples are studied through two or more techniques with images located in the same field of view yielding greater insights than any single technique can offer; correlative microscopy has extraordinary potential for investigating materials properties, particularly their micromechanical characteristics [40].

This review offers an oversight of in-situ optical and non-optical microscopies methods and techniques of taking images to incorporate with DIC, as well as software to improve images with microscopes for DIC to help readers to choose the most suitable corroborative techniques to address important fundamental/applied questions in polymer composite science and engineering with a view to high impact outcomes in technical and medical applications. In the near to medium term, we believe these will be combined with computational approaches to enhance product development in industry (Fig. 2) [41, 42].

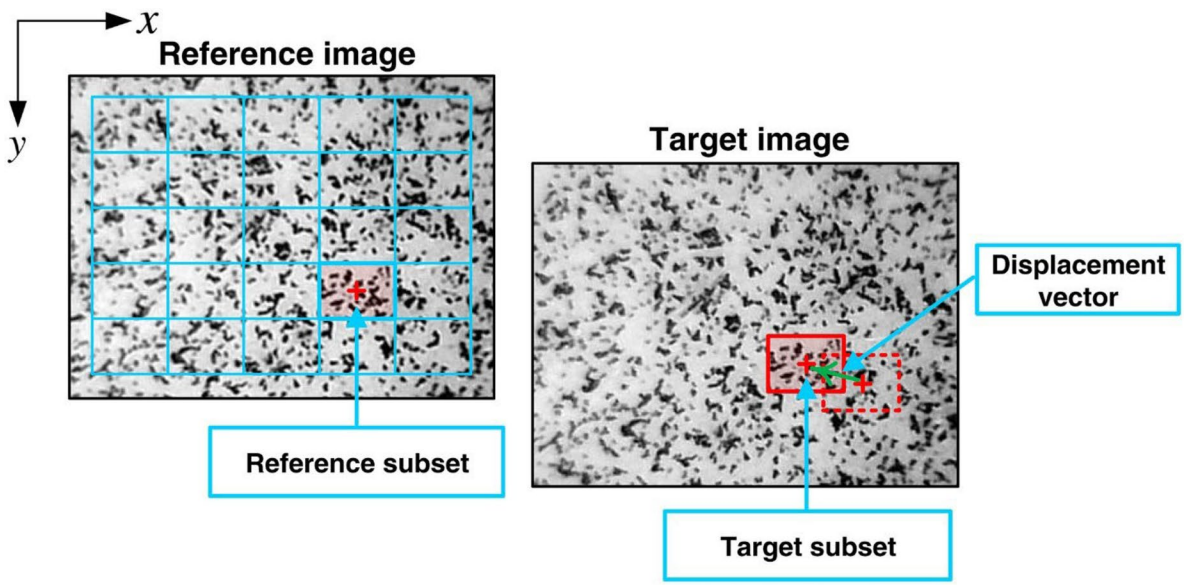

Fig. 1 Schematic illustration of the undeformed subset and the corresponding deformed subset in 2D-DIC. Reproduced from [29] with permission from the publisher (John Wiley and Sons)

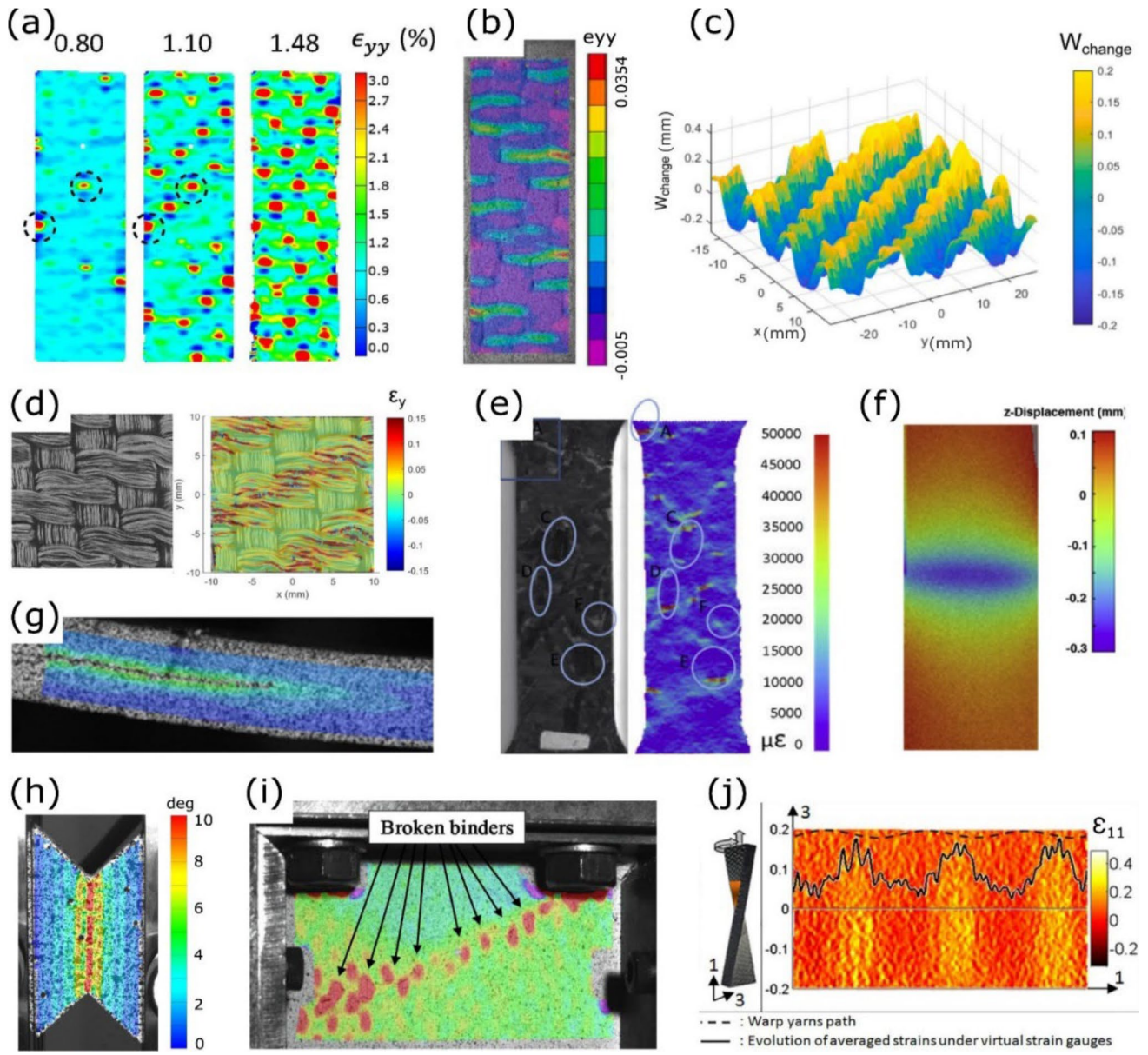

Fig. 2 DIC applications for microscale and mesoscale structure, defects, and damage, **a** strain of z-binders due to failure in 3D woven polymer composite, **b** mesoscale strain concentrations linked to damage development for a 10 mm wide ceramic matrix composite at 900 °C, **c** topographical surface deformation of a twill woven composite, **d** varying local volume fraction within weave resulting in strain concentrations, **e** discontinuous fiber tows strain concentrations at the ends of fiber bundles, **f** delamination detection through out-of-plane motion of laminate composites, **g** crack front propagation observed with 2D-DIC shear strains during end-notch flexure test of carbon/epoxy woven laminate, **h** 30 mm long concentrated shear region influenced by architecture of 3D woven composite, **i** compression after impact for 3D woven composite showing broken z-binders as strain concentrations and (**j**) strain field for combined tension/torsion loading of 3D woven composite showing influence of the weave. Reproduced from [42] with permission from the publisher (Elsevier)

2 In-situ optical microscopy

2.1 Polarized light optical microscopy

Étienne-Louis Malus's pioneering work on light polarization [43, 44], underpinned research and development of applications of polarized light in various scientific and technological fields (including spectroscopy, materials analysis, liquid crystal displays, and optical communication systems) [31, 45–47]. Polarized light is widely used for imaging thin sections of biological tissues (i.e., natural polymer composite materials), often in combination with polarization-sensitive

fluorescence microscopy, polarization-sensitive hyperspectral imaging, polarization-sensitive multiphoton microscopy, etc. [48]. Polarized light optical microscopy (PLM) allows investigation of changes in microscale internal network structure of polymer-based materials caused by deformation [49, 50], furthermore, PLM is a valuable method for detecting and characterizing anisotropy in specimens that influence the polarization plane of light [51]. Cross polarization of light can enhance macroscopic, optical, and surface DIC measurements (Fig. 3) [31]; interesting studies have demonstrated enhanced image contract and mechanical testing using DIC in cellulose nanocrystal films [52] and bat wing skin [53].

2.2 Stereo light microscopy

Stereo-DIC, also known as 3D-DIC [41], works over μm to m length scales with ns time resolution [54]. Stereo light microscopes (SLM) can be used to assist the DIC methods to measure deformation in small-scale sections [55], and stereo-DIC has been used to analyze various composite materials, including fiber-reinforced composites [56, 57], and given their potential in mechanics, materials research, and biological engineering, there is a strong demand for a low-cost, simple, and effective 3D-DIC technique for measuring small object shapes and deformations, which holds significant scientific value [58–64]. A diffraction assisted image correlation (DAIC) method (Fig. 4) can be used with samples ranging from submillimeter to a few centimeters and is much cheaper than existing systems (since both diffracted images are captured with one camera, synchronization issues are eliminated, and DAIC simplifies measurements by relying on diffraction rules for point correspondence, removing the need for intricate calibrations of the imaging system) [65]. Traditional binocular systems use parallax from two cameras for 3D spatial information but face challenges with precision on large objects, their processing algorithms are complicated by lens distortion, transformation, and calibration issues, making high-precision measurements difficult, and a new method utilizing a telecentric camera can circumvent these issues [66].

2.3 Fluorescence microscopy and super-resolution fluorescence microscopy

Fluorescence is a widespread phenomenon utilized, extensively worldwide for a variety of applications [67–69]. Fluorescence microscopy offers users high contrast, non/minimal-invasiveness, minimal preparation requirements, and ease of use [68]. In 2014, three chemists were jointly awarded the Nobel Prize for their contributions to advancing super-resolved fluorescence microscopy [70]. Originally aimed at biological systems by overcoming the diffraction limit of light, super-resolution fluorescence microscopy (SRFM) has now found significant applications in materials science, particularly in

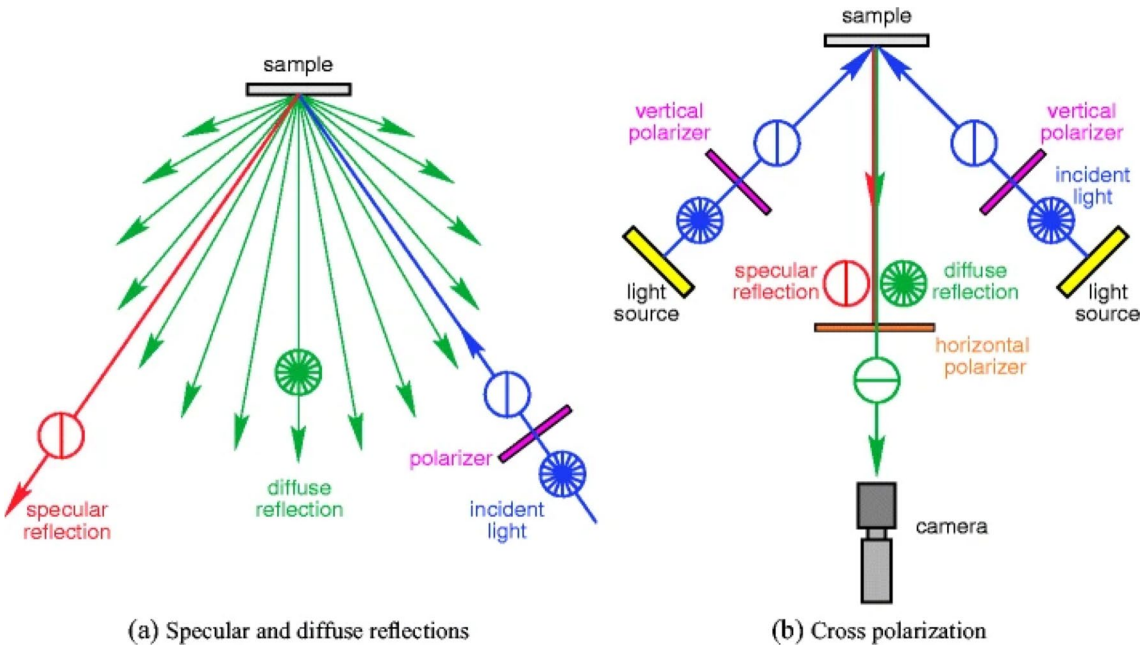

Fig. 3 **a** Specular reflections maintain the polarization of incident light, while diffuse reflections do not. **b** The horizontal polarizer on the camera's lens attenuates the vertically polarized specular reflections to avoid saturated pixels). Reproduced from [31] with permission from the publisher (Springer Nature)

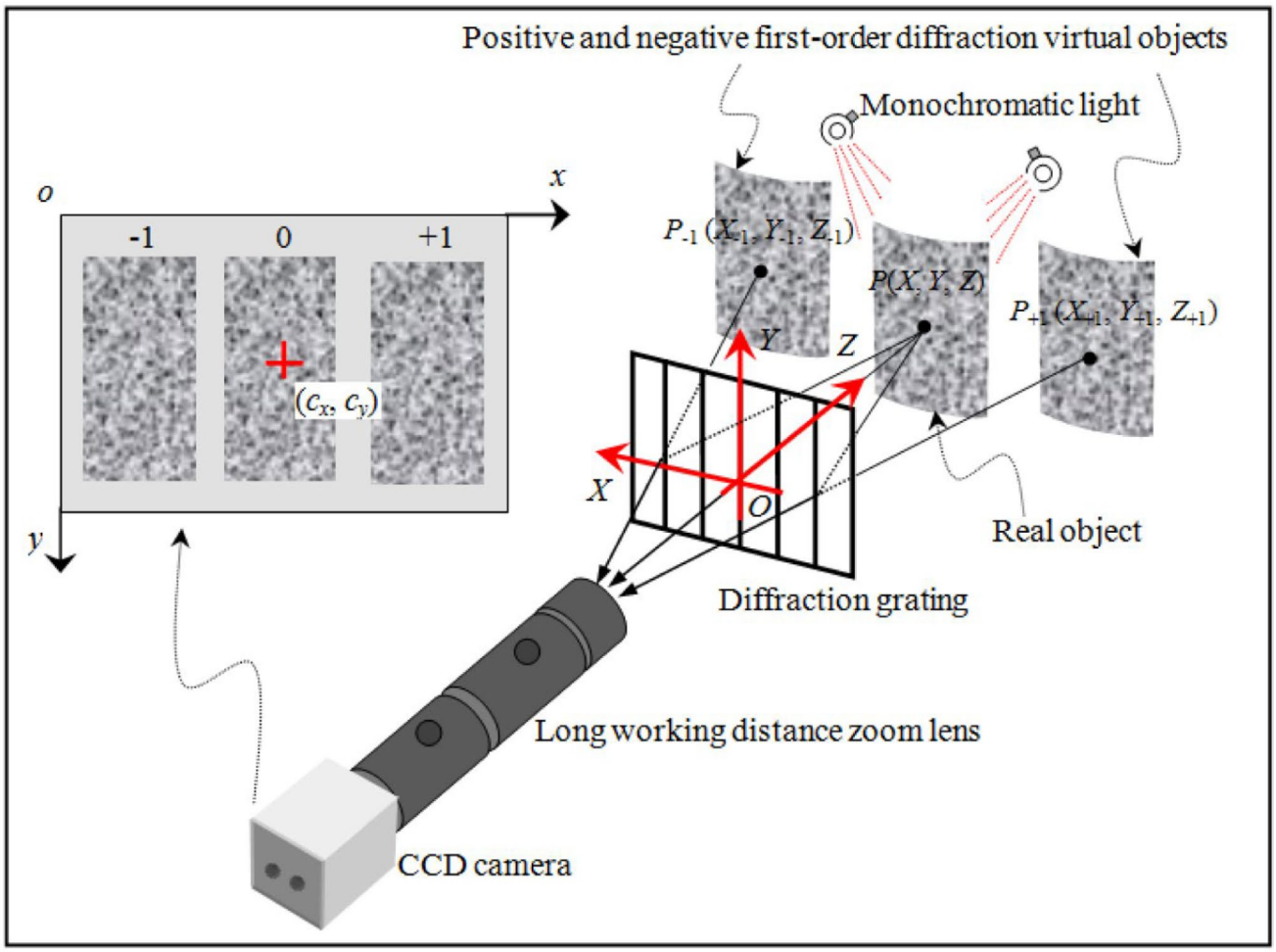

Fig. 4 Schematic diagram of optical arrangement of the single-camera microscopic 3D-DIC method. Reproduced from [65] with permission from the publisher. © 2013 Optical Society of America

polymer research [71, 72]. This shift has prompted a growing number of studies focusing on developing and utilizing new fluorescence visualization techniques to deepen our insights into the specimens under investigation [73, 74]. These new methods include light sheet fluorescence microscopy (LSFM) [75, 76]; photoactivated localization microscopy (PALM) [77–79]; points accumulation for imaging in nanoscale topography (PAINT) [80, 81]; reversible saturable/switchable optical linear fluorescence transitions (RESOLFT) microscopy [82, 83]; single-molecule localization microscopy (SMLM) (Fig. 5) [84–86]; stimulated emission depletion (STED) microscopy [72, 87, 88]; stochastic optical fluctuation imaging (SOFI) [89]; stochastic optical reconstruction microscopy (STORM) and direct STORM (dSTORM) reconstruct the positions of all fluorophores employed to achieve images with a resolution of 20 nm which makes them valuable tools for biological imaging applications [90, 91]; and structured illumination microscopy methods [92]. We have now entered an era where developments in fluorescence imaging strategies (e.g., staining techniques like post-staining following force loading, pre-treatment, and activation of turn-on fluorescence) [79], and quantification methods [93, 94] offer opportunities for super-resolution fluorescence microscopy (SRFM) to investigate the mechanical properties of polymer composite-based materials and deliver exciting results (Fig. 6) [73, 74].

2.4 Confocal laser scanning microscopy (CLSM)

High quality confocal microscopy [95] underpins the mechanical scanning confocal laser microscope [96]. Confocal laser scanning microscopy (CLSM) is applicable to polymer-based materials [97–99], and is utilized by biologists to delineate biological pathways, comprehend intracellular mechanisms, and observe the general structures of living cells [100, 101]; it is capable of high-resolution functional cell imaging, albeit restricted to a depth of about 300 µm [102]. AFM typically offers

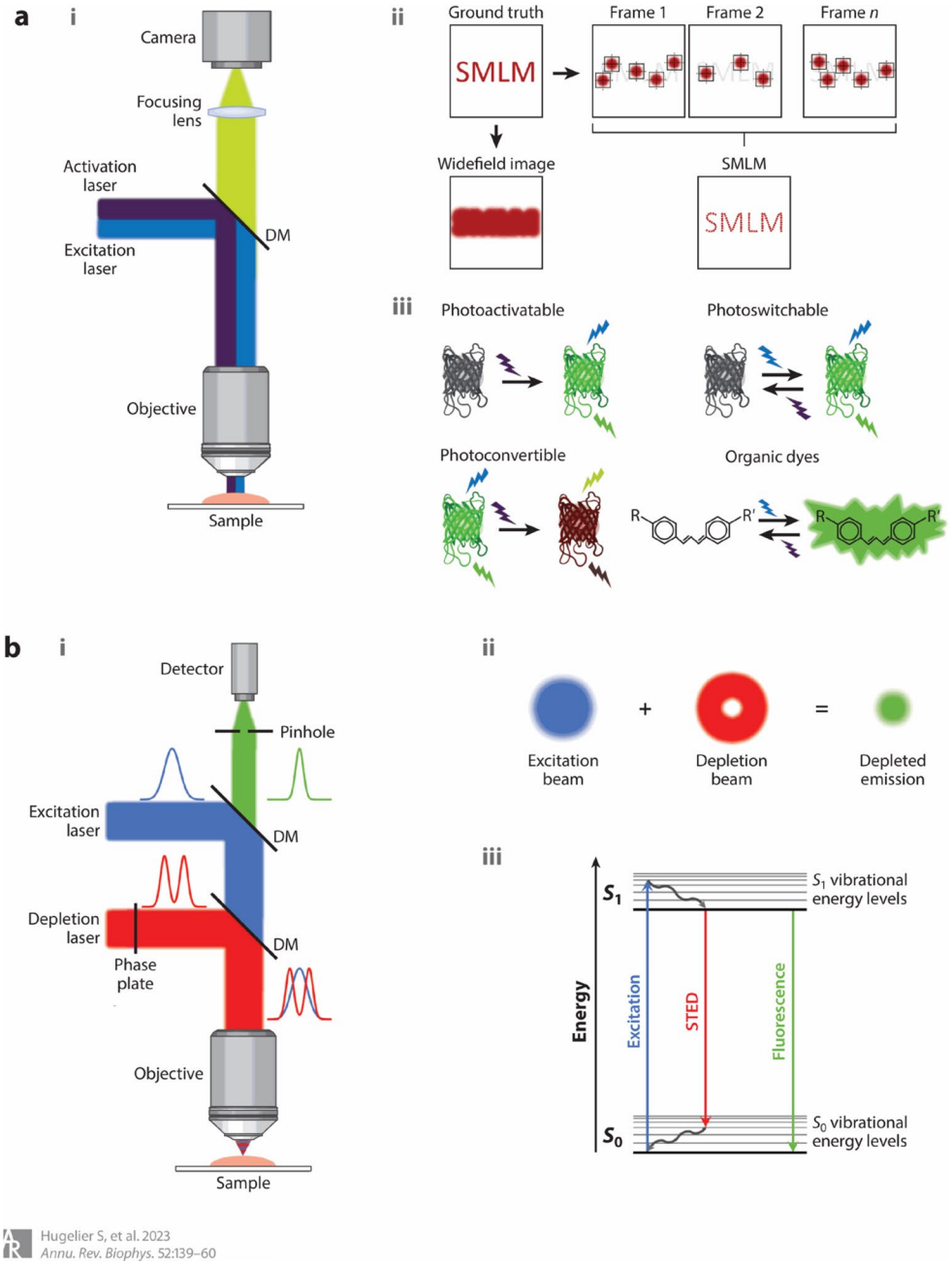

Fig. 5 Schematic representation of the microscope modalities. **a** SMLM. The microscope setup (i), the working principle (ii), and some examples to achieve on/off switching of fluorescent proteins and organic dyes (iii) are shown. **b** STED microscopy. The microscope setup (i), the working principle (ii), and a Jablonski diagram of the STED excitation and emission (iii) are shown. Abbreviations: *DM* dichroic mirror, *SMLM* single-molecule localization microscopy, *STED* stimulated emission depletion. Reproduced from [85] with permission from the publisher (Annual Reviews)

sub 1 nm resolution [103–106], hence, combining AFM and CLSM is interesting for biological applications [100, 101, 107], collecting much more precise 3D images and in-depth analysis of a specimen's structure (Fig. 7) [100–102, 107–110]. One novel technique for improving 3D image capture by LSCM involves combining it with DIC, referred to as the confocal-DIC method [110]; while it is predominantly employed to examine biological samples and colloidal particles [111], it can also aid in characterizing porous structures and nanostructures [112]. Some microscopy-DIC methods are listed in Table 1.

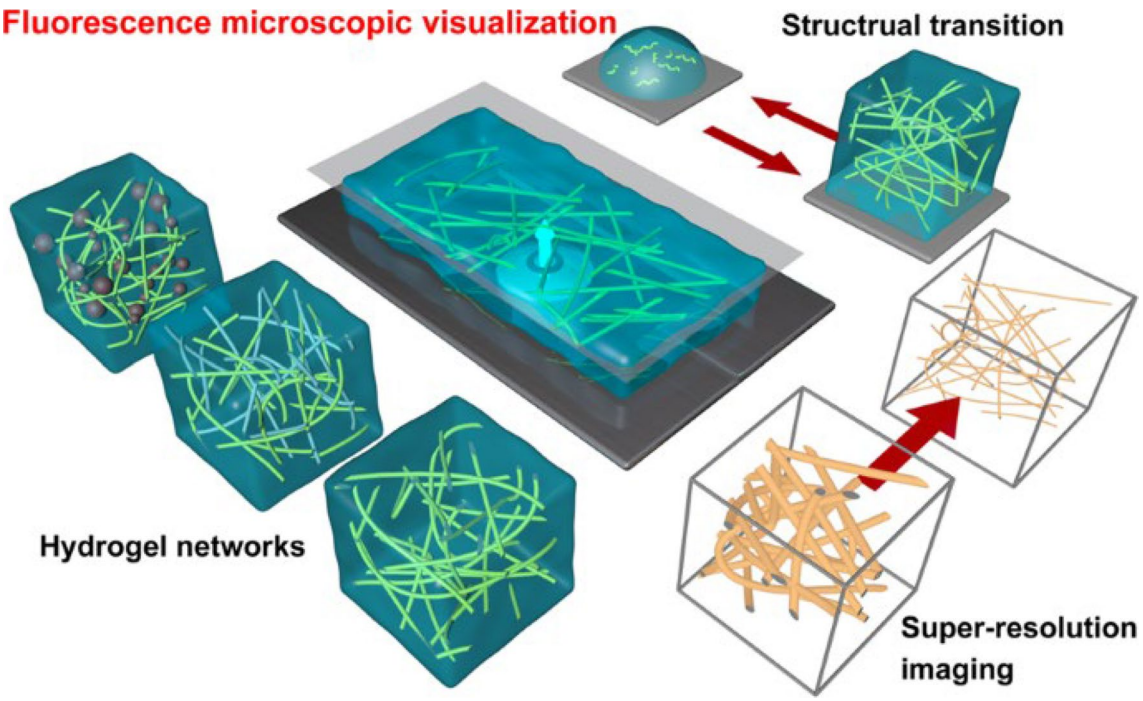

Fig. 6 Schematic illustrating the visualization of different types of hydrogel networks, observation of structural transitions, and super-resolution imaging based on fluorescence microscopy. Reproduced from [73] with permission from the publisher (Springer Nature)

3 In-situ non-optical microscopy

3.1 SEM

SEM images samples over length scales ranging from nm to cm [115], typically via secondary electron imaging (SEI) and backscattered electron imaging (BEI) (Fig. 8) [93]. The application of DIC-SEM is attributed to the synergistic benefits of combining these two powerful techniques, as well as the continuous advancements in the underlying technologies and their increasing accessibility to researchers across various fields [34, 116, 117]. DIC-SEM has been used to study topics such as grain boundary sliding, deformation twinning in materials, crack propagation phase transformations, as well as characterizing the mechanical properties of individual grains, inclusions, and other microstructural features within a material [16, 34, 118–121].

3.2 Transmission electron microscopy (TEM) and scanning transmission electron microscopy (STEM)

TEM is extensively utilized for analyzing and imaging nanoscale samples [31, 115, 122–124]; high-resolution TEM (HRTEM) has a resolution of ≈ 0.5 Å (0.050 nm); cryo-TEM rapidly freezes samples for analysis without inducing changes like agglomeration or deformation. In situ TEM demands special materials—electron-transparent and ultrathin samples—limiting the range of materials tested, with imaging capped at ≈30 frames/second. These techniques necessitate controlled conditions, such as a vacuum SEM/TEM environment, as opposed to reactive air, and recent studies have incorporated DIC measurements in TEM (Fig. 9) [124–126]. STEM merges SEM and TEM modes, has atomic level resolution [127], and has been used to analyze phase separation in polymer blends [128] and a variety of other materials (Fig. 10) [129–135].

3.3 X-ray microscopy

The intricate morphology of many modern materials spans various length scales, requiring multi-scale modeling to understand mechanical behavior from atomic to macroscopic levels [137]. Synchrotron X-ray facilities have improved our

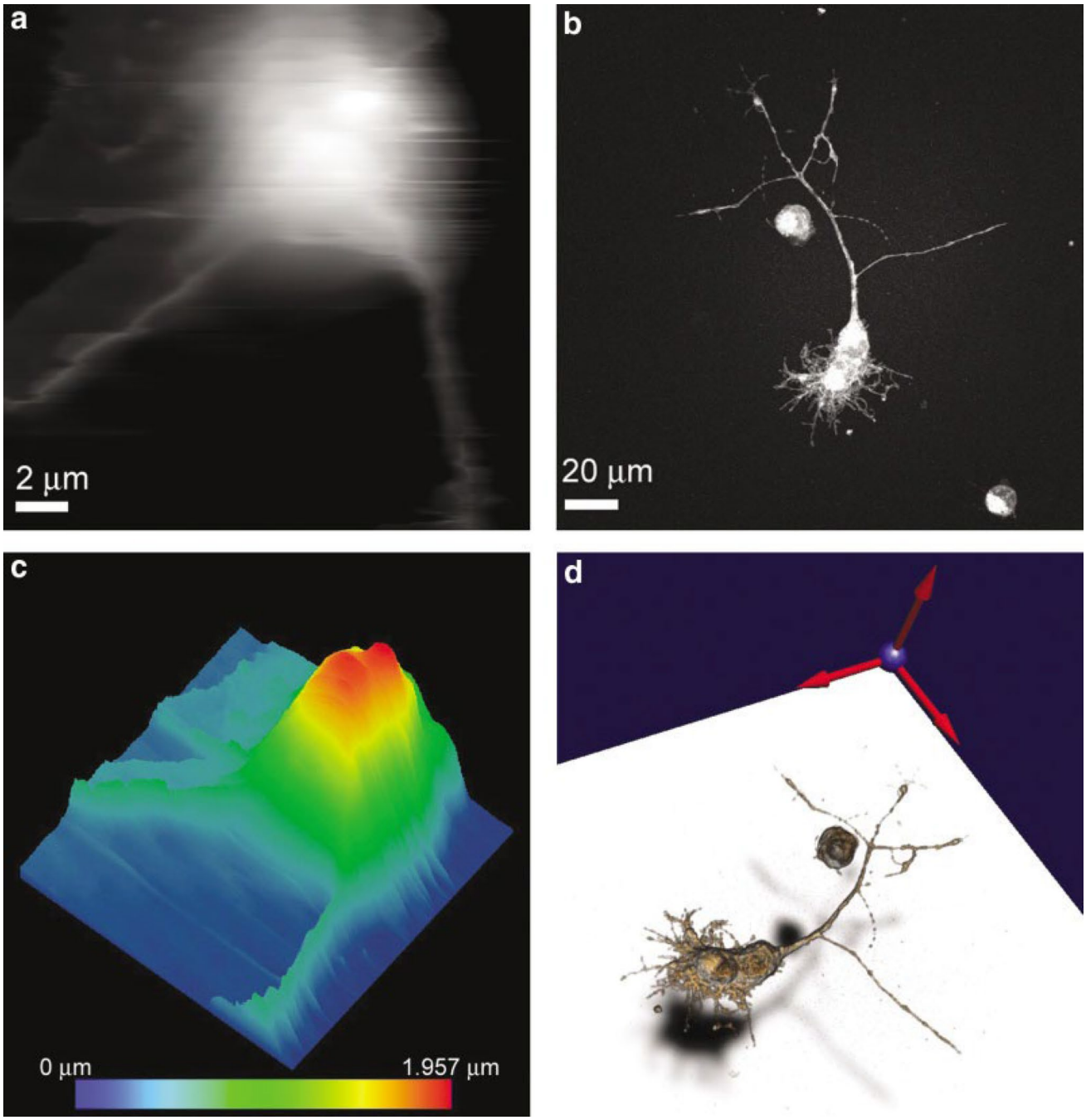

Fig. 7 Examples of visualization of AFM and CLSM data. **a**: AFM range image (gray scale proportional to the elevation); **b**: CLSM maximum intensity projection image; **c**: AFM pseudo-colored isometric view; **d**: CLSM volumetric imaging. The AFM images show the cell body of a live neuronal cell, while CLSM images show the whole live neuron stained with FM 1–43. Reproduced from [101] with permission from the publisher (John Wiley & Sons, Inc.)

ability to study material structures at various length scales using small and wide-angle X-ray scattering (SAXS and WAXS); indeed, in situ mechanical testing in combination with SAXS/WAXS enables the measurement of nanoscale deformations that can be combined with DIC to analyze deformation across multiple length scales simultaneously (Fig. 11) [138–140]. X-ray imaging has transformed microscopy, and in situ soft X-ray Scanning Transmission X-ray Microscopy (STXM) has a spatial resolution of ≈25 nm [126, 141–143] which is applicable to biological samples (Fig. 12); cross-compatibility with CLSM/TEM enables mapping of macromolecule structure/composition through multi-microscopy approaches, which can image complex systems, e.g., biofilms [144]. While advanced microscopy offers many benefits, it can be time-consuming

Table 1 Examples of optical microscopy-DIC methods

Methods	Size/pixels	Techniques	Software	References
Polarized light microscopy + SEM	1–200 µm	Step-and-shoot	Fiji	[49]
Polarized light microscopy + SEM	≈150 µm	PLM/INT	NIS Elements	[50]
Polarized light microscopy	0.73 µm	Cross-polarized		[51]
Stereo light microscopy	2456 × 2058 pixels	Scheimpflug cameras for 3D microscopic DIC	Ncorr	[54]
Stereo light microscope	0.063 × 0.063 mm	2D DIC (MDIC)	Elite Software	[113]
Light sheet fluorescence microscopy (LSFM)	532/580 nm	OptoRheo	ImageJ/Fiji	[76]
Confocal microscopy	0.5 µm	Hand-drawn contouring system	SURPASS, Leica LAS X 3D, IMARIS	[114]

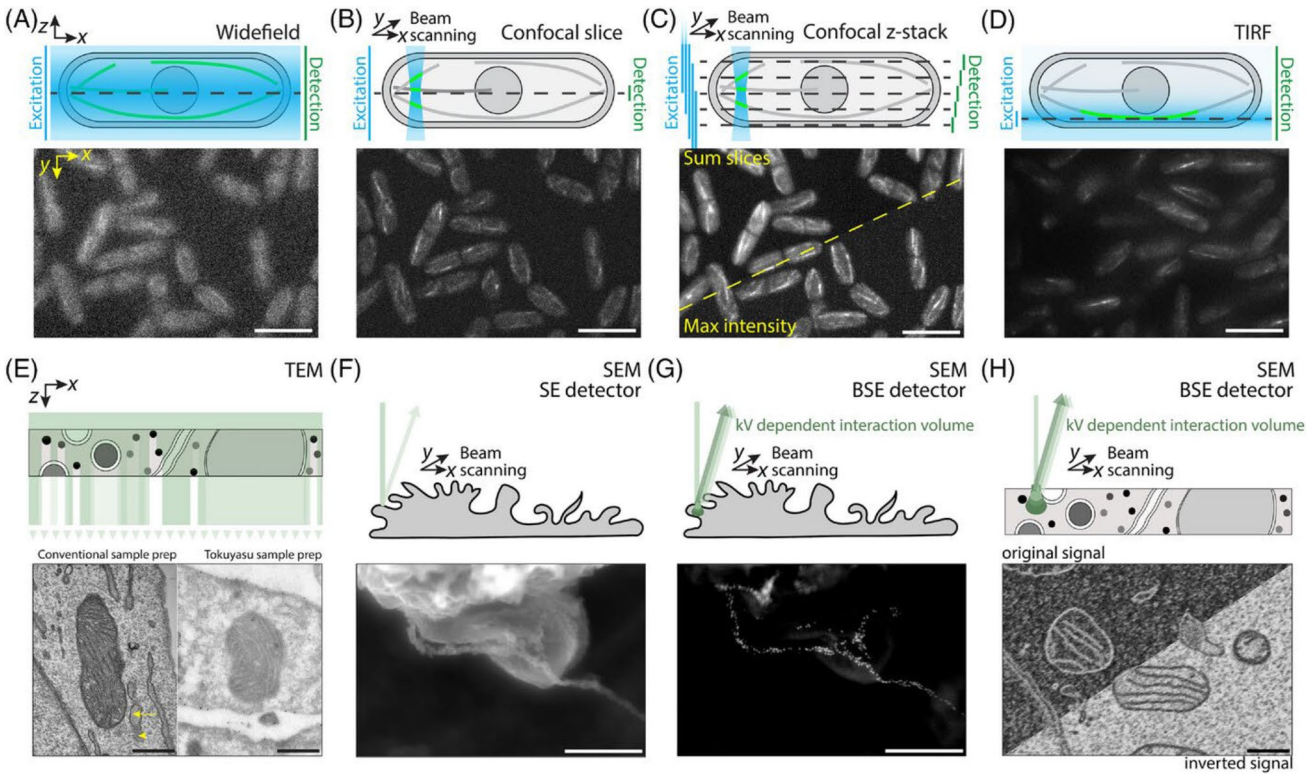

Fig. 8 Image formation in fluorescence and electron microscopy. **A** Widefield microscopy captures live *Schizosaccharomyces pombe* cells expressing sfGFP-tubulin, illuminating the entire sample volume simultaneously. Out-of-focus fluorescence can obscure fine details. **B** Confocal microscopy scans individual diffraction-limited laser spots (laser-scanning) or sweeps them (spinning disk) to avoid out-of-focus light, enhancing contrast and detail across sample depths. **C** Confocal slices can be compiled into a 3D 'z-stack', which can be projected as a single image through summed or maximum intensity values. **D** TIRF microscopy employs an evanescent field that illuminates only a few hundred nanometers from the coverslip, capturing fluorescence primarily from structures near the coverslip, differing from (**A**)–(**C**). All fluorescence scale bars = 10 µm. **E** TEM reveals mitochondria in a thin embedded section, comparing different preparation protocols: conventional (electron dense) and Tokuyasu (electron lucent). Tokuyasu image by I. J. White. **F** SEM detects exocytosis events on endothelial cells, visualizing Von Willebrand factor strings. **G** SEM with backscattered electron detection highlights gold-labelled antibodies on Von Willebrand factor. Images by K. O'Neill and D. Cutler. **H** SEM with BSE of a resin-embedded thin section shows heavy metal areas producing stronger signals (light) compared to lighter regions. This method often inverts data for clearer comparison, with green ellipses indicating interaction volumes of the electron beam at varying voltages. All EM scale bars = 500 nm. Reproduced reference [93] with permission from the publisher (John Wiley & Sons)

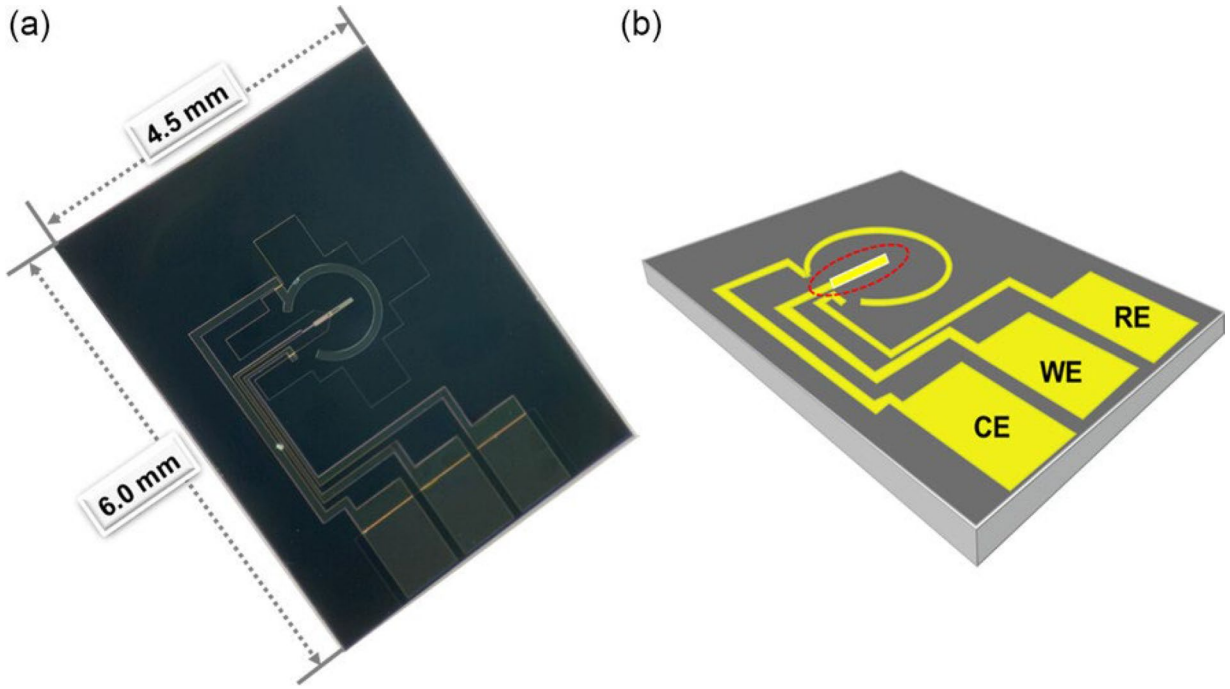

Fig. 9 Picture of the in situ electrochemical TEM chip. **a** Schematic view of the in situ electrochemical TEM chip, and **b** the viewing window was indicated by the red dashed circle. Reproduced from [136] with permission from the publisher (John Wiley and Sons)

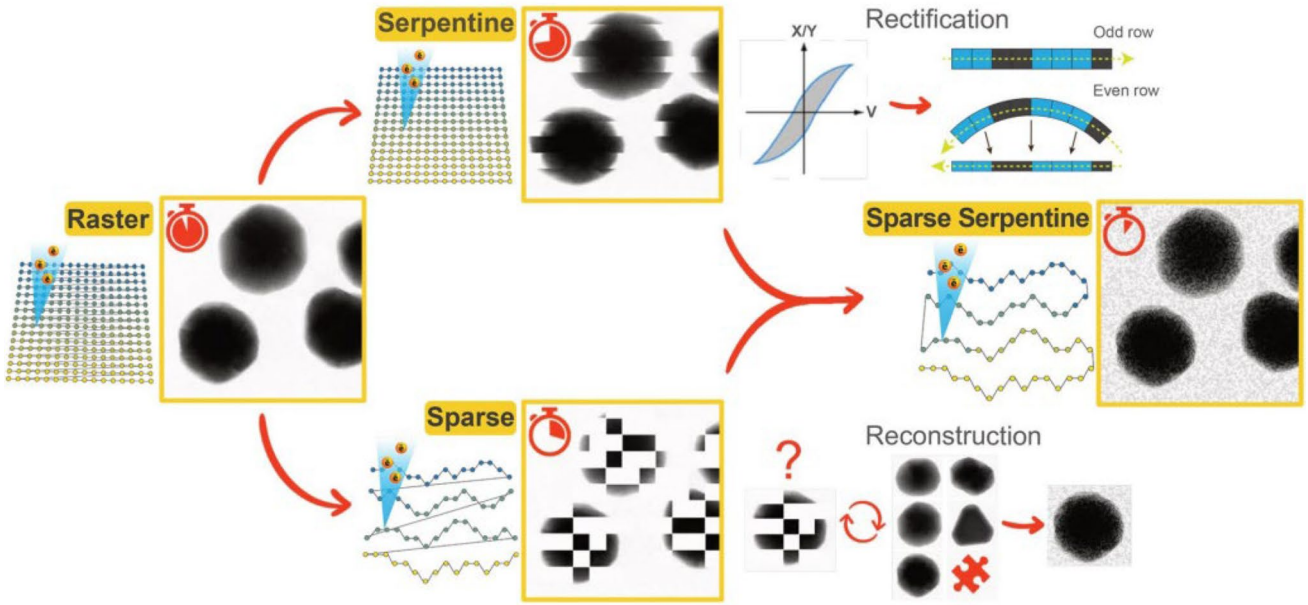

Fig. 10 Schematic illustration of different scanning strategies and their relative acquisition time. The standard pixel-by-pixel raster scan of Scanning Transmission Electron Microscopy (STEM) includes the addition of a 'flyback' time to relocate the beam at the beginning of the next row. Via a serpentine scan, the frame rate can be improved by avoiding any dead time τ, but the rectification of odd and even rows is required to compensate for hysteresis effects of the magnetic scan coils. Sparse imaging results in the recording of fewer pixels through a random-walk scan thus reduce the total time. Here, a reconstruction algorithm is needed to "inpaint" the full frame. Both approaches can be combined to achieve the highest possible STEM image acquisition speed while avoiding an increase in electron dose. Reproduced from [134] with permission from the publisher (Springer Nature)

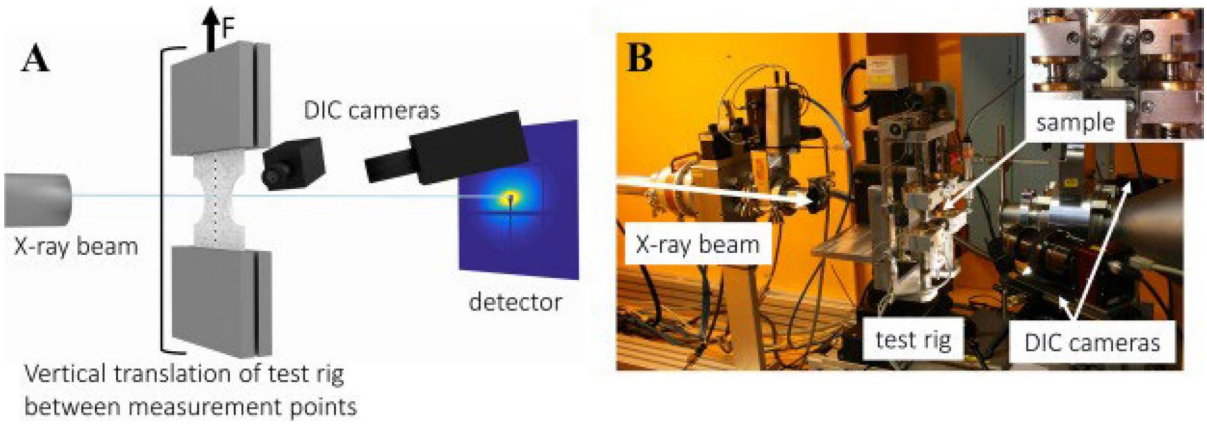

Fig. 11 Experimental setup. **A** Schematic illustration of a sample tested in tension and simultaneously monitored with DIC and SAXS or WAXS at 10 discrete vertical positions in the horizontal-centre of the sample. The sample is subjected to continuous tensile loading in the test rig and the whole rig is translated vertically to move the sample between the measurement points inside the beam. **B** Photograph of the experimental setup at the I911-4 beamline (MAX IV Laboratory, Lund University, Lund, Sweden). Reproduced from [138] with permission from the publisher (Elsevier BV)

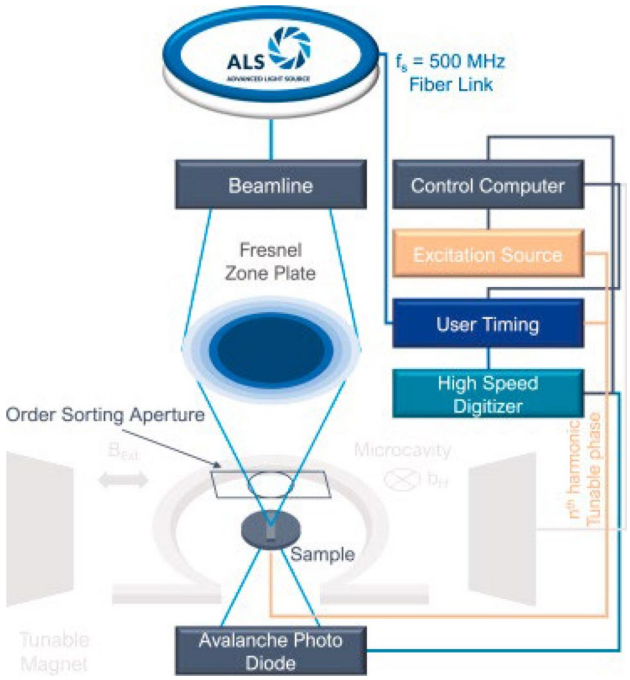

Fig. 12 Schematic representation of the TR-STXM setup realized at ALS beamline 11.0.2.2. The STXM is situated in a high-vacuum chamber. Gray colored parts are optional components for (dynamic) magnetic measurements. Reproduced from [142] with permission from the publisher (Elsevier BV)

and involve complex digital image algorithms [145]; new software like STXM_deconv helps users with limited image processing skills [146], and Gaussian mixture (GM) and Bayesian Gaussian mixture (BGM) clustering methods operate based on similarity and proximity rather than traditional algorithms [147]. Employing these strategies demonstrates X-ray microscopy's ability to enable mapping and analyzing elemental structures, aiding DIC method in investigating the chemical/micromechanical properties of polymer-based materials.

3.4 Atomic force microscopy (AFM)

Atomic Force Microscopy (AFM) has nm scale resolution via a surface probe technique that enables topographical and nanomechanical measurements (potentially under physiological conditions) [103, 148] and recent advances enabled studies of multiparametric heterogeneity of materials [149, 150]. Combination with Total Internal Reflection Fluorescence Microscopy (TIRFM) [151] and Scanning Near-Field Optical Microscopy (SNOM/NSOM) [152] has enabled interesting

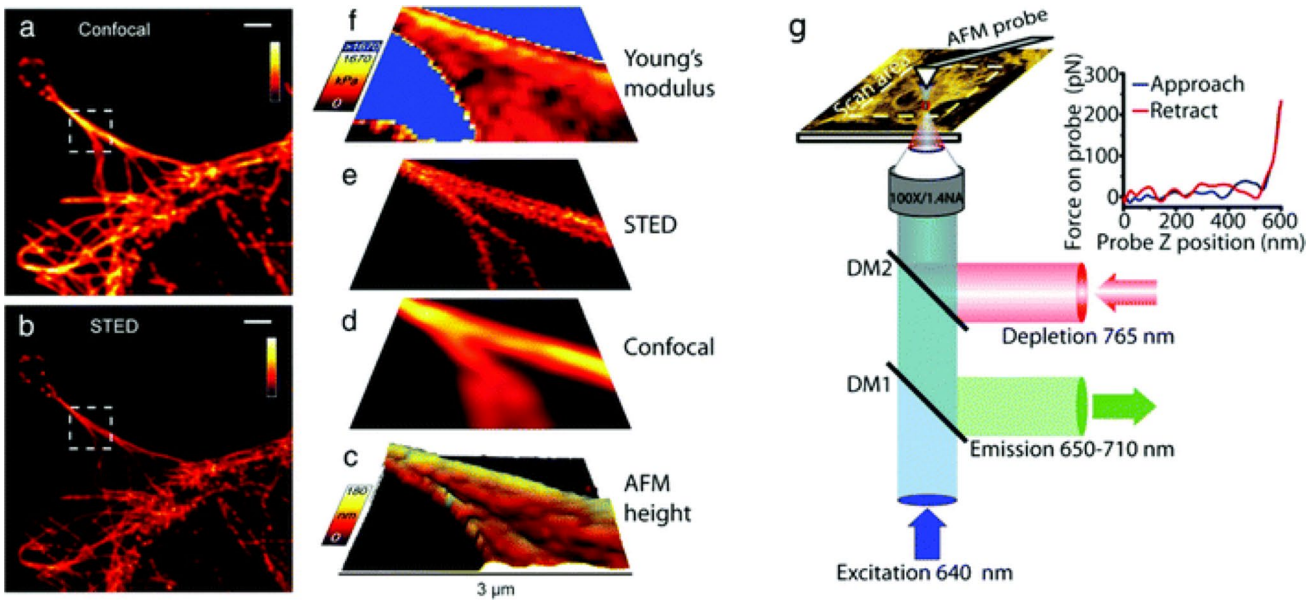

Fig. 13 **a**–**f** Correlative AFM + STED imaging of Cos7 cells labelled with Atto 647 N. **a** Confocal raw image, **b** STED raw image, **c** 3D rendered view of AFM measured height extracted from AFM force curves, deconvolved (**d**) confocal and (**e**) STED images, and (**f**) an elasticity map calculated from AFM force curves. **g** Schematic diagram of a combined AFM/STED imaging set-up. The AFM cantilever is aligned such that STED and AFM have a common scan area. Fluorescence excitation pulses are combined with depletion pulses using a dichroic mirror (DM2), and fluorescent emission is separated using a dichroic mirror (DM1). AFM images are acquired by translating the sample. For each pixel a force curve is measured by approaching the tip toward the sample and recording the tip–sample interaction force as a function of the cantilever z-position (see inset), and the Young's modulus is estimated from the gradient. Scale bars in (**a** and **b**): 2 µm. (**a**–**f**). Reproduced from [150] with permission from the publisher (Royal Society of Chemistry)

biological applications, e.g., (Fig. 13). It has also been possible to demonstrate simultaneous imaging and nanomanipulation [149, 150]. Some non-optical microscopes-DIC methods are listed in Table 2.

4 Software

The DIC methodology employed for measuring mechanical properties involves image acquisition, processing, and correlation; free and commercial software have been created for analysis of DIC data, examples of which are listed in Table 3 [52, 113, 159–164]. These resources are versatile and can be utilized across various research fields where understanding structure–property relationships are of critical importance, and we foresee them playing an increasingly important role in research and development in academia and industry (Fig. 14).

5 Combination with other techniques

The exciting properties of natural/synthetic composites highlights the importance of understanding their mechanical behavior [167]. DIC can analyze the behavior of such composites under different loads and moreover, be combined with other mechanical methods for greater insights [168], where DIC provides high-resolution images and insights about the micromechanical characteristics of such materials [169]. The combination of DIC and finite element analysis (FEA) has been used to investigate dentin micromechanics [170] or those of human soft tissues [171], to conducting fatigue tests on composites [172], to study distributed fiber optic sensors (DFOS) in concrete structures [173], or indeed small punch tests (SPT) for specimen mapping [174]. Nanoindentation measurements are well established in the analysis of polymer-based materials and their composites [175–178]. A nanoindentation method allows for local mechanical characterization of materials at micro and nanometer scales; this technique has been applied across diverse fields, including biology, engineering, geology and materials science [167, 179]; however, despite

Table 2 Non-optical microscopy-DIC methods

Methods	Size/pixels	Detector	Software	Techniques	References
SEM	25 × 25 pixels		ARAMIS	BEI, SEI	[34]
SEM		Air brush	GOM Correlate	SENT	[118]
SEM	Micro scale	Electron backscattering diffraction (EBSD)	GOM Correlate	HKL channel 5	[119]
SEM	micro-scale	A backscattered electron (BSE)	Avizo v2020	Operando	[153]
Focused ion beam (FIB)	10–15 nm			Liquid gallium (Ga)	[154]
SEM	≈1 µm	Back Scattered (BSD), Secondary Electron (SED)	VIC-2D software	Step-and-shoot	[120, 155]
SEM	≈10 nm	Secondary electron emission, back scattered electron emission	Wolfram Mathematica §R 10	Stereo pair	[121]
SEM	≈10 nm	MD (mirror detector) for BSE imaging	CASINO V2.51	Very low voltage (VLV)	[156]
STEM + X-ray ptychography	128 × 128 pixels	(EMPAD)		Annular dark field (ADF)	[157]
SEM		SE, BSE, EBSD, EDS	VEDDAC		[158]
TEM	≈2 nm	Laplacian of Gaussian (LoG)	VIC-2D	Particle Tracking (PT)	[124]
STEM	512 × 512 pixels	High angle annular dark field (HAADF)	Nuxutra Image-Inpainting	Nuxutra Image-Inpainting, Fiji ImageJ, Digital Micrograph	[134]
STEM	(≈0–40 mrad)	Annular dark field (ADF)	STEMsim software package	High angle scattering of electrons captured	[135]
STXM	25 nm			Operando	[126]
STXM (three types)	< 1 mm			Talbot-carpet	[143]
DIC-SAXS/WAXS	300 × 300 µm^2	PILATUS 2 M	ImageJ v1.50i/VIC-3D7	plugin OrientationJ	[138]

Table 3 Examples of DIC Software

Software	Commercial/ open source	Implement	Institute/company	Application	References
ARAMIS	Commercial	Python		Uniform illumination of the specimen surface	[113, 159]
CorreliSTC	Commercial		Airbus Group Innovations	2D, 3D	[159]
Dantec Dynamics	Commercial	MATLAB		2D, 3D	[163]
Eikosim	Commercial	MATLAB		2D, 3D	[163]
Elite		Python		2D, 3D	[113]
GOM	Commercial	C++, MATLAB		3D	[159–163]
ISI-Sys VIC	Commercial	C++, MATLAB		2D, 3D	[160]
LaVision StrainMaster	Commercial	MATLAB	Max Planck Institute and Laser Laboratory in Gottingen	2D, 3D	[159, 161–163]
MatchID-2D	Commercial	MATLAB		2D, 3D	[159, 162, 163]
Q-400	Commercial		Dantec Dynamics	3D	[159]
TEMA	Commercial			2D, 3D	[159]
VEDDAC	Commercial			3D	[158]
Vic-2D	Commercial		Correlated Solutions Inc, USA	2D displacements	[120, 155] [159, 161]
Video Gauge™	Commercial		Imetrum	High stress, crack opening or other discontinuities	[159]
ALDIC	Open source	MATLAB		2D	[161–163]
ADIC2D	Open source	MATLAB		2D	[162, 163]
ADIC3D	Open source	MATLAB		3D	[163]
Avizo v2020	Open source	MATLAB		3D	[153]
DIC Engine (DICe)	Open source	C++	Sandia National Laboratories, Albuquerque, New Mexico	GUI 2D, 3D	[159–163]
Digital Micrograph	Open source	MATLAB	Gatan Ametek, CA, USA- University of Wollongong, NSW, Australia	2D	[134]
dolfin_dic	Open source	Python	École Polytechnique, Palaiseau, France	2D, 3D	[159]
iCorrVision-2D	Open source	Python		2D, material characterization, perform J -Integral, kinematic parameters, investigate the deformation homogeneity of mechanical samples	[162]
iCorrVision-3D	Open source	Python		3D	[163]
ImageJ	Open source	MATLAB	Wayne Rasband, National Institute of Health, Bethesda, MD, USA	2D, 3D	[76, 153, 165]
MultiDIC	Open source	MATLAB		3D	[163]
NCorr	Open source	MATLAB C++	Georgia Institute of Technology, Atlanta, Georgia	Graphical User Interface (GUI), 2D, behavior of the foam under compression	[54, 153, 159–163, 166]
NIS Elements 4.0			Laboratory imaging, Czech Republic		[50]
PReDIC	Open source	MATLAB		2D	[163]
pydic	Open source	Python	University of Limoges, Limoges, France		[159, 161]

Table 3 (continued)

Software	Commercial/ open source	Implement	Institute/company	Application	References
py2DIC	Open source	Python	(University of Rome La Sapienza, Rome, Italy	GUI 2D	[159, 161–163]
pyxel	Open source	Python	Institut National des Sciences Appliquées de Toulouse, Toulouse, France	Mechanics, 2D	[159]
RealPi2dDIC	Open source	Python		2D	[161–163]
µDIC	Open source	Python		2D	[160–163]
Ufreckles	Open source	MATLAB		2D	[161, 163]
YaDICs	Open source	C+ +	Laboratoire de Mécanique de Lille, Lille, France	Kinematics, 2D, 3D	[159, 162, 163]
YADICS	Open source	MATLAB		2D	[161–163]

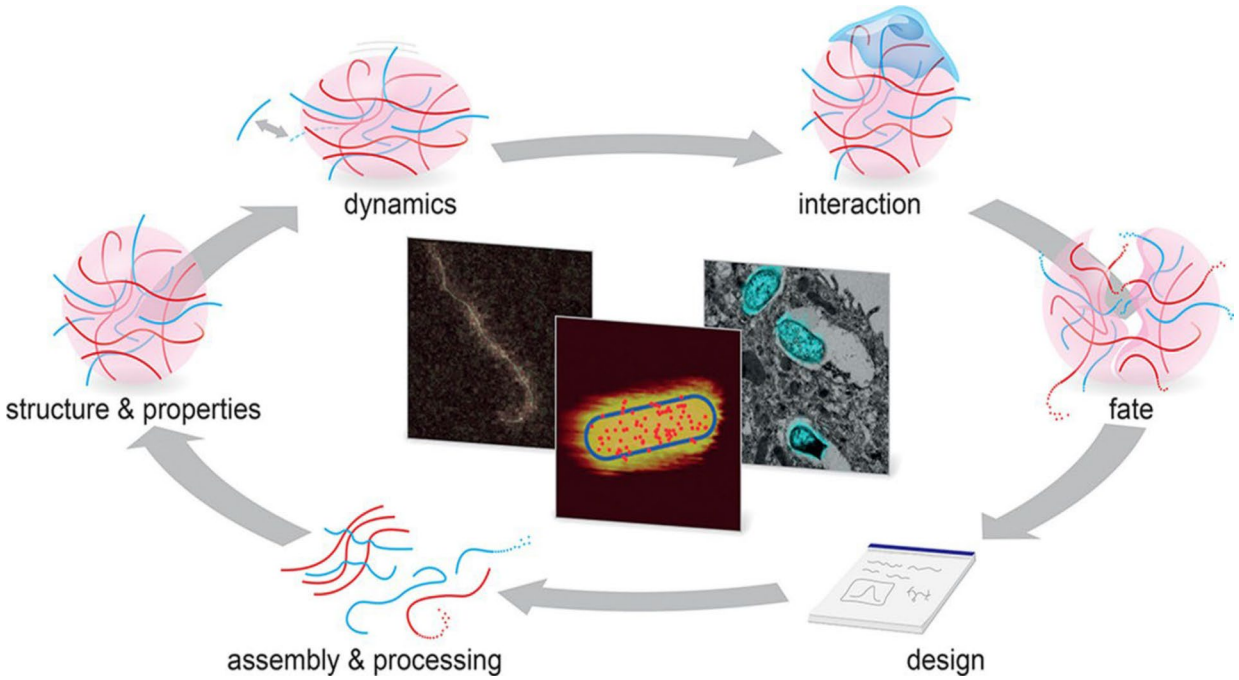

Fig. 14 Steps in the life cycle of polymeric materials that correlative microscopy can contribute to study and understand. Reproduced from [40] with permission from the publisher (John Wiley & Sons)

its widespread use, this method cannot independently account for the elastic, hardness [179, 180], and chemical [181–183] properties of shale due to the inherent complexity of the source rocks, but the combination with DIC can effectively resolve these issues. Some 3D imaging technologies (e.g., computed tomography (CT) [184–187], etc.) combined with DIC algorithms offer opportunities assess internal displacement/deformation information of materials-digital volume correlation (DVC), this is becoming increasingly important in the field of analyzing material microstructures, and we point the interested reader towards excellent review articles [188–191]. Some examples of DIC combined other techniques are listed in Table 4.

6 Conclusion

The mechanical properties of polymer-based materials is one of the factors that make them ubiquitous in our everyday lives [3, 4]. DIC can be integrated with both traditional and innovative techniques to validate and enhance mechanical testing studies, providing deeper insights into the material's characteristics and factors influencing them. While effective in controlled lab settings, DIC studies undertaken in natural environments are challenging owing to a variety of complications including uneven illumination, shadows, blurring, and noise, which can hinder its effectiveness and may be addressed in future research. In this review we highlight the viability of both optical and non-optical microscopic methods for obtaining high-quality images using DIC across various length and time scales which have attracted significant

Table 4 Examples of application of DIC combined with other techniques to analyse composites

Combination methods	DIC measure	Combined-method measure	Microscopy	Specimen	References
DIC-FEA	Strain	Stress	Optical	Dentin	[170]
DIC-fatigue test	Map strain	Stiffness/absorb energy		E-glass fiber	[172]
DIC-DFOS	Strain	Crack monitoring	Optical	Concrete structures	[173]
DIC-SPT	Elastic and plastic	Tensile	Optical	Steel	[174]
DIC-Nanoindentation	Elastic/hardness		SEM	Rocks	[179, 180]
DIC-Nanoindentation	Stiffness	Viscoelasticity	AFM	Composite	[167]

attention from researchers in academia and industry. We believe such techniques will play an important role in the future of materials science and engineering [192]; indeed DIC is one of a variety of computational approaches that can be applied to generate large datasets to feed into models that enable the development and production of advanced materials to precisely designed properties potentially employing AI/ML approaches to facilitate this [193, 194].

Authors contributions Conceptualisation: S.M. Methodology (literature search and data analysis): S.M. Writing—original draft preparation: S.M. and J.G.H. Writing—review and editing: S.M. and J.G.H. Funding acquisition: J.G.H. Supervision: J.G.H.

Funding We thank the Engineering and Physical Sciences Research Council (EPSRC, EP/R003823/1, EP/R511560/1) and the Royal Society (RG160449) for financial support.

Data availability Not applicable.

Code availability Not applicable.

Declarations

Competing interests The authors declare no competing interests.

References

1. Das R, Karumbaiah K M. Biodegradable polyester-based blends and composites: manufacturing, properties, and applications. Biodegrad Polyes. 2015;11:321–40.
2. Chen Z, Lin Y-T, Salehi H, Che Z, Zhu Y, Ding J, Sheng B, Zhu R, Jiao P. Advanced fabrication of mechanical metamaterials based on micro/nanoscale technology. Adv Eng Mat. 2023. https://doi.org/10.1002/adem.202370075.
3. Ravichandran M, et al. Recent developments in polymer matrix composites–a review. IOP Conf Ser Mater Sci Eng. 2020. https://doi.org/10.1088/1757-899X/988/1/012096.
4. Oladele IO, Omotosho TF, Adediran AA. Polymer-based composites: an indispensable material for present and future applications. Int J Poly Sci. 2020;2020(1):8834518.
5. Collar EP, García-Martínez J-M. Mechanical behavior of polymeric materials: recent studies. Polymers. 2024;16(19):2821.
6. Laverty R. The shift from phenomenological to physics-based modeling of polymers: 2024 benjamin franklin medal in mechanical engineering presented to Mary C. Boyce, Ph. D. J Franklin Inst. 2024. https://doi.org/10.1016/j.jfranklin.2024.107375.
7. Ali A, et al. Carbon nanotube characteristics and enhancement effects on the mechanical features of polymer-based materials and structures–a review. J Market Res. 2023;24:6495–521.
8. Grediac M. The use of full-field measurement methods in composite material characterization: interest and limitations. Compos A Appl Sci Manuf. 2004;35(7–8):751–61.
9. Moeendarbary E, Harris AR. Cell mechanics: principles, practices, and prospects. Wiley Interdiscipl Rev: Syst Biol Med. 2014;6(5):371–88.
10. Liang X. Visualization of nanomechanical properties of polymer composites using atomic force microscopy. Polym J. 2023;55(9):913–20.
11. Venkateshaiah A, et al. Microscopic techniques for the analysis of micro and nanostructures of biopolymers and their derivatives. Polymers. 2020;12(3):512.
12. Majerczak K, et al. Polyhydroxybutyrate: a review of experimental and simulation studies of the effect of fillers on crystallinity and mechanical properties. Polym Int. 2022;71(12):1398–408.
13. Fouda I, Shabana H. Opto-mechanical properties of fibres. Part 1. Optical properties and orientation of drawn polyethylene fibres. Polymer Int. 1999;48(3):181–8.
14. Fouda I, Shabana H. Opto-mechanical properties of fibres. Part 2. Effect of stretching on some optical and structure parameters of PET fibres (woollen type). Polymer Int. 1999;48(3):189–97.
15. Tsukruk VV, et al. Dynamic microprobing of viscoelastic polymer properties. Polym Int. 2000;49(5):441–4.
16. Weidner A, Biermann H. Review on strain localization phenomena studied by high-resolution digital image correlation. Adv Eng Mater. 2021;23(4):2001409.
17. Khoo S-W, Karuppanan S, Tan C-S. A review of surface deformation and strain measurement using two-dimensional digital image correlation. Metrol Measurement Syst. 2016;23(3):461–80.

18. Chen B, Coppieters S. Unified digital image correlation under meshfree framework. Strain. 2024;60(1): e12461.
19. Brüster B, et al. In situ multiscale study of deformation heterogeneities in polylactide-based materials upon drawing: Influence of initial crystallinity and plasticization. J Polym Sci, Part B: Polym Phys. 2018;56(21):1452–68.
20. Huynh NU, Koohbor B, Youssef G. Light-matter interactions revealing load-induced phase mobility in elastomers. Macromol Rapid Commun. 2023;44(7):2200725.
21. Hubbard AM, et al. Shape memory polymers for self-folding via compression of thermoplastic sheets. J Appl Polym Sci. 2018;135(47):46889.
22. Truszkiewicz E, et al. Mechanical behavior of 3D-printed polymeric metamaterials for lightweight applications. J Appl Polym Sci. 2022;139(6):51618.
23. Chen F, et al. Exploring digital image correlation technique for the analysis of the tensile properties of all-cellulose composites. Cellulose. 2021;28:4165–78.
24. Han R, et al. Effects of crosslinking densities on mechanical properties of nitrile rubber composites in thermal oxidative aging environment. J Appl Polym Sci. 2020;137(36):49076.
25. Fu L, et al. The effect of loading rate on the interfacial behavior of overmolded hybrid fiber reinforced polypropylene composites. J Appl Polym Sci. 2021;138(47):51390.
26. Ayadi A, et al. Large-scale X-ray microtomography analysis of fiber orientation in weld line of short glass fiber reinforced thermoplastic and related elasticity behavior. Macromol Mater Eng. 2016;301(8):907–21.
27. Ritchie L, Pahl E, Anderson IA. The incompressibility assumption and piezoresistivity in stretchable conductive composites. J Appl Polymer Sci. 2024. https://doi.org/10.1002/app.55855.
28. Sigrüner M, et al. Pull-out behavior of polymer fibers in concrete. J Polym Sci. 2023;61(21):2708–20.
29. Zhao J, Sang Y, Duan F. The state of the art of two-dimensional digital image correlation computational method. Eng Rep. 2019;1(2): e12038.
30. Berfield T, et al. Micro-and nanoscale deformation measurement of surface and internal planes via digital image correlation. Exp Mech. 2007;47:51–62.
31. LePage WS, Daly SH, Shaw JA. Cross polarization for improved digital image correlation. Exp Mech. 2016;56:969–85.
32. Dong Y, Pan B. A review of speckle pattern fabrication and assessment for digital image correlation. Exp Mech. 2017;57:1161–81.
33. Lionello G, Cristofolini L. A practical approach to optimizing the preparation of speckle patterns for digital-image correlation. Meas Sci Technol. 2014;25(10): 107001.
34. Jin H, Lu W-Y, Korellis J. Micro-scale deformation measurement using the digital image correlation technique and scanning electron microscope imaging. J Strain Anal Eng Design. 2008;43(8):719–28.
35. Hoefnagels JP, Van Maris M, Vermeij T. One-step deposition of nano-to-micron-scalable, high-quality digital image correlation patterns for high-strain in-situ multi-microscopy testing. Strain. 2019;55(6): e12330.
36. Thokchom AK, Shin S. Dynamical clustering and band formation of particles in a marangoni vortexing droplet. Langmuir. 2019;35(27):8977–83.
37. Githens A, Daly S. Patterning corrosion-susceptible metallic alloys for digital image correlation in a scanning electron microscope. Strain. 2017;53(1): e12215.
38. Yan D, Tasan CC, Raabe D. High resolution in situ mapping of microstrain and microstructure evolution reveals damage resistance criteria in dual phase steels. Acta Mater. 2015;96:399–409.
39. van Beeck J, et al. Quantification of three-dimensional surface deformation using global digital image correlation. Exp Mech. 2014;54:557–70.
40. Wang Y, et al. Correlative imaging for polymer science. J Polym Sci. 2021;59(12):1232–40.
41. McDonagh JL, et al. What can digitisation do for formulated product innovation and development? Polym Int. 2021;70(3):248–55.
42. Holmes J, et al. Digital image and volume correlation for deformation and damage characterisation of fibre-reinforced composites: a review. Compos Struct. 2023;315: 116994.
43. Paris, S.t.p.d., *Bulletin de la Société philomathique de Paris*. 1826. 85.
44. Paris, S.t.p.d., *Bulletin de la Société philomathique de Paris. Fondée en 1788, c.1 ser.2 1810–11*. 1826. 299.
45. Brosseau, C., *Fundamentals of polarized light: a statistical optics approach.* (No Title), 1998.
46. Scharf T. Polarized light in liquid crystals and polymers. Hoboken: John Wiley & Sons; 2007.
47. Andrews DL. Photonics, volume 1: fundamentals of photonics and physics. Hoboken: John Wiley & Sons; 2015.
48. Alali S, Vitkin A. Polarized light imaging in biomedicine: emerging Mueller matrix methodologies for bulk tissue assessment. J Biomed Opt. 2015;20(6):061104–061104.
49. Verschatse O, et al. In-situ observations of microscale ductility in a quasi-brittle bulk scale epoxy. Polymers. 2020;12(11):2581.
50. Slouf M, et al. In situ observation of nucleated polymer crystallization in polyoxymethylene sandwich composites. Front Mat. 2015;2:23.
51. Turčanová M, et al. Full-range optical imaging of planar collagen fiber orientation using polarized light microscopy. Biomed Res Int. 2021;2021(1):6879765.
52. Diaz JA, et al. Thermal expansion of self-organized and shear-oriented cellulose nanocrystal films. Biomacromol. 2013;14(8):2900–8.
53. Skulborstad AJ, et al. Polarized image correlation for large deformation fiber kinematics. Exp Mech. 2013;53:1405–13.
54. Sun C, et al. Scheimpflug camera-based stereo-digital image correlation for full-field 3D deformation measurement. J Sens. 2019;2019(1):5391827.
55. Liu X, Lu R. Testing system for the mechanical properties of small-scale specimens based on 3d microscopic digital image correlation. Sensors. 2020;20(12):3530.
56. Holmes J, et al. Characterisation of off-axis tensile behaviour and mesoscale deformation of woven carbon-fibre/PEEK using digital image correlation and X-ray computed tomography. Compos B Eng. 2022;229: 109448.
57. Cao M, et al. Progressive failure of inter-woven carbon-Dyneema fabric reinforced hybrid composites. Compos Struct. 2019;211:175–86.
58. Hu Y, et al. Calibration and rectification of bi-telecentric lenses in Scheimpflug condition. Opt Lasers Eng. 2022;149: 106793.
59. Wang M, et al. Improved performance of multi-view fringe projection 3D microscopy. Opt Express. 2017;25(16):19408–21.

60. Li, J., et al. *A detailed design model based on trust chain for seam tracking system of gas metal arc welding*. in *The 2nd International Conference on Information Science and Engineering*. 2010. IEEE.
61. Wang P, et al. The extraction of depth information about the object based on binocular vision. Sci Technol Eng. 2014;14(002):56–61.
62. Guo H, et al. Calibration of binocular vision measurement of large gear workpiece welding. J Donghua Univ Sci. 2013;4:455–9.
63. Chen Z, Liao H, Zhang X. Telecentric stereo micro-vision system: calibration method and experiments. Opt Lasers Eng. 2014;57:82–92.
64. Chen Z, et al. Precision alignment of optical fibers based on telecentric stereo microvision. IEEE/ASME Trans Mechatron. 2016;21(4):1924–34.
65. Pan B, Wang Q. Single-camera microscopic stereo digital image correlation using a diffraction grating. Opt Exp. 2013;21(21):25056–68.
66. Zhang S, et al. High-precision measurement of binocular telecentric vision system with novel calibration and matching methods. ieee access. 2019;7:54682–92.
67. Valeur B, Berberan-Santos MN. Molecular fluorescence: principles and applications. Hoboken: John Wiley & Sons; 2013.
68. Kubitscheck U. John Fluorescence microscopy: from principles to biological applications. Hoboken: Wiley & Sons; 2017.
69. Su W, et al. Research progress review of preparation and applications of fluorescent hydrogels. J Chem. 2020;2020(1):8246429.
70. Möckl, L., D.C. Lamb, and C. Bräuchle, 2014. *Super-resolved fluorescence microscopy: Nobel Prize in Chemistry 2014 for Eric Betzig, Stefan Hell, and William E. Moerner.* Angewandte Chemie International Edition, **53**(51).
71. Birk UJ. Super-resolution microscopy: a practical guide. Hoboken: John Wiley & Sons; 2017.
72. Birk UJ. Stimulated emission depletion microscopy, in super-resolution microscopy: a practical guide. Hoboken: John Wiley & Sons; 2017.
73. Zhong J, Zhao T, Liu M. Fluorescence microscopic visualization of functionalized hydrogels. NPG Asia Materials. 2022;14(1):38.
74. Nevskyi O, Wöll D. 3D super-resolution fluorescence imaging of microgels. Annu Rev Phys Chem. 2023;74(1):391–414.
75. Reynaud EG, Tomancak P. Light sheet fluorescence microscopy. Hoboken: John Wiley & Sons; 2024.
76. Mendonca T, et al. OptoRheo: simultaneous in situ micro-mechanical sensing and imaging of live 3D biological systems. Commun Biol. 2023;6(1):463.
77. Sengupta P, Lippincott-Schwartz J. Quantitative analysis of photoactivated localization microscopy (PALM) datasets using pair-correlation analysis. BioEssays. 2012;34(5):396–405.
78. Henriques R, et al. PALM and STORM: unlocking live-cell super-resolution. Biopolymers. 2011;95(5):322–31.
79. Shroff H, White H, Betzig E. Photoactivated localization microscopy (PALM) of adhesion complexes. Current Prot Cell Biol. 2013. https://doi.org/10.1002/0471143030.cb0421s58.
80. Maity BK, et al. Peptide-PAINT using a transfected-docker enables live-and fixed-cell super-resolution imaging. Small Meth. 2023;7(4):2201181.
81. Delcanale P, et al. Nanoscale mapping functional sites on nanoparticles by points accumulation for imaging in nanoscale topography (PAINT). ACS Nano. 2018;12(8):7629–37.
82. Bodén A, et al. Super-sectioning with multi-sheet reversible saturable optical fluorescence transitions (RESOLFT) microscopy. Nature Meth. 2024. https://doi.org/10.1038/s41592-024-02196-8.
83. Roubinet B, et al. Carboxylated photoswitchable diarylethenes for biolabeling and super-resolution RESOLFT microscopy. Angew Chem Int Ed. 2016;55(49):15429–33.
84. Scalisi S, Pisignano D, Cella Zanacchi F. Single-molecule localization microscopy goes quantitative. Microscopy Res Techn. 2023;86(4):494–504.
85. Hugelier S, Colosi P, Lakadamyali M. Quantitative single-molecule localization microscopy. Annu Rev Biophys. 2023;52(1):139–60.
86. Shi, W., S. Fu, and Y. Li, 2023. High-throughput single-molecule localization microscopy: Potential clinical applications. Clinical and Translational Medicine, **13**(4).
87. Li C, et al. Stimulated emission depletion microscopy. eLS. 2021;2:1–8.
88. Wu Z, Xu X, Xi P. Stimulated emission depletion microscopy for biological imaging in four dimensions: a review. Microsc Res Tech. 2021;84(9):1947–58.
89. Peeters Y, et al. Correcting for photodestruction in super-resolution optical fluctuation imaging. Sci Rep. 2017;7(1):10470.
90. Xu J, Ma H, Liu Y. Stochastic optical reconstruction microscopy (STORM). Cur Prot Cytometry. 2017;81(1):12–46.
91. Jensen E, Crossman DJ. Technical review: types of imaging—direct STORM. Anat Rec. 2014;297(12):2227–31.
92. Hannebelle MT, et al. Open-source microscope add-on for structured illumination microscopy. Nat Commun. 2024;15(1):1550.
93. Culley S, et al. Made to measure: an introduction to quantifying microscopy data in the life sciences. J Microsc. 2024;295(1):61–82.
94. Hamilton N. Quantification and its applications in fluorescent microscopy imaging. Traffic. 2009;10(8):951–61.
95. Diaspro, A., *Confocal and two-photon microscopy: foundations, applications and advances*. 2001: Whily.
96. Chang, G.-W., et al. *Optomechanical analysis for confocal laser scanning microscopes*. in *Optomechanics 2005*. 2005. SPIE.
97. Bayguinov PO, et al. Modern laser scanning confocal microscopy. Curr Protoc Cytom. 2018;85(1): e39.
98. Elliott AD. Confocal microscopy: principles and modern practices. Curr Protoc Cytom. 2020;92(1): e68.
99. Abbasi Moud A. Polymer blends analyzed with confocal laser scanning microscopy. Polym Bull. 2023;80(6):5929–64.
100. McNally HA, et al. Comparative three-dimensional imaging of living neurons with confocal and atomic force microscopy. J Neurosci Methods. 2005;142(2):177–84.
101. Rajwa B, et al. AFM/CLSM data visualization and comparison using an open-source toolkit. Microsc Res Tech. 2004;64(2):176–84.
102. Belay B, et al. Optical projection tomography as a quantitative tool for analysis of cell morphology and density in 3D hydrogels. Sci Rep. 2021;11(1):6538.
103. Haugstad G. Atomic force microscopy: understanding basic modes and advanced applications. Hoboken: John Wiley & Sons; 2012.
104. Gavara N. A beginner's guide to atomic force microscopy probing for cell mechanics. Microsc Res Tech. 2017;80(1):75–84.
105. Cascione M, et al. Atomic force microscopy combined with optical microscopy for cells investigation. Microsc Res Tech. 2017;80(1):109–23.
106. Umeda K, McArthur SJ, Kodera N. Spatiotemporal resolution in high-speed atomic force microscopy for studying biological macromolecules in action. Microscopy. 2023;72(2):151–61.
107. Kondra S, et al. Integration of confocal and atomic force microscopy images. J Neurosci Methods. 2009;177(1):94–107.

108. Franck C, et al. Three-dimensional full-field measurements of large deformations in soft materials using confocal microscopy and digital volume correlation. Exp Mech. 2007;47:427–38.
109. Bhat SV, et al. Correlative atomic force microscopy quantitative imaging-laser scanning confocal microscopy quantifies the impact of stressors on live cells in real-time. Sci Rep. 2018;8(1):8305.
110. Yang Y, Souare PM, Sylvestre J. Using confocal microscopy and digital image correlation to measure local strains around a chip corner and a crack front. IEEE Trans Device Mater Reliab. 2019;20(1):97–105.
111. Mohraz A, Solomon MJ. Direct visualization of colloidal rod assembly by confocal microscopy. Langmuir. 2005;21(12):5298–306.
112. Oyarzún DP, et al. Atomic force microscopy (AFM) and 3D confocal microscopy as alternative techniques for the morphological characterization of anodic TiO2 nanoporous layers. Mater Lett. 2016;165:67–70.
113. Paysan F, Dietrich E, Breitbarth E. A robot-assisted microscopy system for digital image correlation in fatigue crack growth testing. Exp Mech. 2023;63(6):975–86.
114. Fernández-Iglesias Á, et al. A simple method based on confocal microscopy and thick sections recognizes seven subphases in growth plate chondrocytes. Sci Rep. 2020;10(1):6935.
115. Dehm G, Howe JM, Zweck J. In-situ electron microscopy: applications in physics, chemistry and materials science. Hoboken: John Wiley & Sons; 2012.
116. Kammers A, Daly S. Small-scale patterning methods for digital image correlation under scanning electron microscopy. Meas Sci Technol. 2011;22(12): 125501.
117. Goulmy JP, et al. Classification of the acquisition conditions driving the accuracy of strain measurements during in situ DIC with scanning electron microscope. Strain. 2024;60(1): e12456.
118. Daelemans L, et al. Toughening mechanisms responsible for excellent crack resistance in thermoplastic nanofiber reinforced epoxies through in-situ optical and scanning electron microscopy. Compos Sci Technol. 2021;201: 108504.
119. Li M-Y, et al. Detecting the deformation behavior of bimodal Ti-6Al-4V using a digital image correlation technique. Materials. 2022;15(21):7504.
120. Verschatse O, et al. Development of a versatile speckle pattern of nano-sized polymer particles for high-resolution SEM-DIC. Polym Testing. 2023;125: 108134.
121. Henao-Londoño J, et al. 3D Stereo reconstruction of SEM images. Modern Appl Sci. 2018;12(12):57–64.
122. De Hosson JTM. Advances in transmission electron microscopy: In situ straining and in situ compression experiments on metallic glasses. Microsc Res Tech. 2009;72(3):250–60.
123. Li J, Wang Z, Hufnagel T. Characterization of nanometer-scale defects in metallic glasses by quantitative high-resolution transmission electron microscopy. Phys Rev B. 2002;65(14): 144201.
124. Zhang Y, et al. Full-field deformation measurements in the transmission electron microscope using digital image correlation and particle tracking. Mater Charact. 2022;183: 111598.
125. Amer M, et al. A review on in situ mechanical testing of coatings. Coatings. 2022;12(3):299.
126. Prabu V, et al. Instrumentation for in situ flow electrochemical scanning transmission X-ray microscopy (STXM). Rev Sci Inst. 2018. https://doi.org/10.1063/1.5023288.
127. *Scanning Transmission Electron Microscopy*, in *Handbook of Microscopy Set: Applications in Materials Science, Solid-State Physics and Chemistry: Vols. 1+2+3*, D.v.D. Prof. S. Amelinckx, J. van Landuyt, G. van Tendeloo, Editor. 1996.
128. Pal R, et al. Study of polycarbonate–polystyrene interfaces using scanning transmission electron microscopy spectrum imaging (STEM-SI). Polym Int. 2023;72(1):106–12.
129. Tyukalova E, Duchamp M. Atomic resolution enabled STEM imaging of nanocrystals at cryogenic temperature. J Phy: Mat. 2020;3(3): 034006.
130. Houben L, Heidelmann M, Gunkel F. Spatial resolution and radiation damage in quantitative high-resolution STEM-EEL spectroscopy in oxides. Micron. 2012;43(4):532–7.
131. Leijten Z, et al. Low-dose (S) TEM elemental analysis of water and oxygen uptake in beam sensitive materials. Ultramicroscopy. 2020;208: 112855.
132. Zhou L, et al. Low-dose phase retrieval of biological specimens using cryo-electron ptychography. Nat Commun. 2020;11(1):2773.
133. Sang X, et al. Precision controlled atomic resolution scanning transmission electron microscopy using spiral scan pathways. Sci Rep. 2017;7(1):43585.
134. Ortega E, et al. High temporal-resolution scanning transmission electron microscopy using sparse-serpentine scan pathways. Sci Rep. 2021;11(1):22722.
135. Beyer A, et al. Influence of plasmon excitations on atomic-resolution quantitative 4D scanning transmission electron microscopy. Sci Rep. 2020;10(1):17890.
136. Han, Z., et al., , 2024 Quasi-in situ Observation of MnO2 Nanorods by Electrochemical Transmission Electron Microscopy for Oxygen Reduction Reaction Process. Advanced Energy and Sustainability Research. p. 2300229.
137. Mota-Santiago P, et al. In situ biaxial loading and multi-scale deformation measurements of nanostructured materials at the CoSAXS beamline at MAX IV Laboratory. J Appl Crystallogr. 2023;56(4):967–75.
138. Gustafsson A, et al. Linking multiscale deformation to microstructure in cortical bone using in situ loading, digital image correlation and synchrotron X-ray scattering. Acta Biomater. 2018;69:323–31.
139. Salvati E, et al. Multiscale analysis of bamboo deformation mechanisms following NaOH treatment using X-ray and correlative microscopy. Acta Biomater. 2018;72:329–41.
140. Birmpilis G, et al. Monitoring of the nano-structure response of natural clay under mechanical perturbation using small angle X-ray scattering and digital image correlation. Acta Geotech. 2019;14:1965–75.
141. Wood, C. and E. Duke, X-ray vision: Transforming microscopy through advanced imaging techniques. 2024.
142. Feggeler T, et al. Scanning transmission X-ray microscopy at the advanced light source. J Elect Spectrosc Relat Phenom. 2023;267: 147381.
143. Günther B, et al. Full-field structured-illumination super-resolution X-ray transmission microscopy. Nat Commun. 2019;10(1):2494.

144. Lawrence J, et al. Scanning transmission X-ray, laser scanning, and transmission electron microscopy mapping of the exopolymeric matrix of microbial biofilms. Appl Environ Microbiol. 2003;69(9):5543–54.
145. Lühl L, et al. Scanning transmission X-ray microscopy with efficient X-ray fluorescence detection (STXM-XRF) for biomedical applications in the soft and tender energy range. J Synchrotron Radiat. 2019;26(2):430–8.
146. Ornelas JL, et al. STXMdeconv-a MATLAB Script for the Deconvolution of STXM Images. Microsc Microanal. 2018;24(S2):120–1.
147. De La Rosa N, et al. Clustering methods for the characterization of synchrotron radiation X-Ray fluorescence images of human carotid atherosclerotic plaque. Adv Intel Syst. 2024;6(9):2400052.
148. Allison DP, et al. Atomic force microscopy of biological samples. Wiley Interdisciplinary Rev: Nanomed Nanobiotechnol. 2010;2(6):618–34.
149. Gómez-Varela AI, et al. Simultaneous co-localized super-resolution fluorescence microscopy and atomic force microscopy: combined SIM and AFM platform for the life sciences. Sci Rep. 2020;10(1):1122.
150. Miranda A, et al. How did correlative atomic force microscopy and super-resolution microscopy evolve in the quest for unravelling enigmas in biology? Nanoscale. 2021;13(4):2082–99.
151. Sanderson J. Understanding light microscopy. Hoboken: John Wiley & Sons; 2019.
152. Beversluis MR, Stranick SJ. Scanning near-field optical microscopy. Charact Mater. 2002. https://doi.org/10.1002/0471266965.com153.
153. Statnik ES, et al. Multi-scale digital image correlation analysis of in situ deformation of open-cell porous ultra-high molecular weight polyethylene foam. Polymers. 2020;12(11):2607.
154. Herráez M, et al. Microscale characterization techniques of fibre-reinforced polymers. In: Peter W, editor., et al., The Structural Integrity of Carbon Fiber Composites. Cham: Springer International Publishing; 2017. p. 283–99.
155. Verschatse O, et al. Microscale and macroscale deformation behavior of electrospun polymeric nanofiber membranes using in situ sem during mechanical testing. Polymers. 2023;15(7):1630.
156. Zarraoa L, González MU, Paulo ÁS. Imaging low-dimensional nanostructures by very low voltage scanning electron microscopy: ultra-shallow topography and depth-tunable material contrast. Sci Rep. 2019;9(1):16263.
157. Chen Z, et al. Mixed-state electron ptychography enables sub-angstrom resolution imaging with picometer precision at low dose. Nat Commun. 2020;11(1):2994.
158. Qayyum F, et al. Examining the effect of MnS particles on the local deformation behavior of 8MnCrS4-4-13 steel by in situ tensile testing and digital image correlation. J Comp Sci. 2023;7(7):294.
159. Belloni V, et al. py2DIC: a new free and open source software for displacement and strain measurements in the field of experimental mechanics. Sensors. 2019;19(18):3832.
160. Olufsen SN, Andersen ME, Fagerholt E. µDIC: an open-source toolkit for digital image correlation. SoftwareX. 2020;11: 100391.
161. Das PP, et al. RealPi2dDIC: a low-cost and open-source approach to in situ 2D digital image correlation (DIC) applications. SoftwareX. 2021;13: 100645.
162. de Deus Filho JCA, da Silva Nunes LC, Xavier JMC. iCorrVision-2D: an integrated python-based open-source digital image correlation software for in-plane measurements (Part 1). SoftwareX. 2022;19: 101131.
163. Nunes L, Xavier J. iCorrVision-3D: an integrated python-based open-source digital image correlation software for in-plane and out-of-plane measurements (Part 2). SoftwareX. 2022;19: 101132.
164. Garcia, D., et al. 2013. A generic synthetic image generator package for the evaluation of 3D Digital Image Correlation and other computer vision-based measurement techniques. in PhotoMechanics 2013.
165. Delp A, et al. In situ characterization of polycaprolactone fiber response to quasi-static tensile loading in scanning electron microscopy. Polymers. 2021;13(13):2090.
166. Blaber J, Adair B, Antoniou A. Ncorr: open-source 2D digital image correlation matlab software. Exp Mech. 2015;55(6):1105–22.
167. Gonabadi H, et al. Investigation of the effects of environmental fatigue on the mechanical properties of GFRP composite constituents using nanoindentation. Exp Mech. 2022;62(4):585–602.
168. Fayyad TM, Lees JM. Application of digital image correlation to reinforced concrete fracture. Procedia Mat Sci. 2014;3:1585–90.
169. Mousa MA, et al. A digital image correlation technique for laboratory structural tests and applications: a systematic literature review. Sensors. 2023;23(23):9362.
170. Wang W, et al. A new method combining finite element analysis and digital image correlation to assess macroscopic mechanical properties of dentin. Materials. 2015;8(2):535–50.
171. Moerman KM, et al. Digital image correlation and finite element modelling as a method to determine mechanical properties of human soft tissue in vivo. J Biomech. 2009;42(8):1150–3.
172. Giancane S, et al. Fatigue damage evolution of fiber reinforced composites with digital image correlation analysis. Procedia Eng. 2010;2(1):1307–15.
173. Herbers M, et al. Crack monitoring on concrete structures: comparison of various distributed fiber optic sensors with digital image correlation method. Struct Concr. 2023;24(5):6123–40.
174. Vijayanand V, et al. A novel methodology for estimating tensile properties in a small punch test employing in-situ DIC based deflection mapping. J Nucl Mater. 2020;538: 152260.
175. VanLandingham MR, et al. Nanoindentation of polymers: an overview. Macromol Symposia. 2001;167(1):15.
176. Gibson RF. A review of recent research on nanoindentation of polymer composites and their constituents. Compos Sci Technol. 2014;105:51–65.
177. Shen, Y.-L., Nanoindentation for testing material properties. In: Handbook of Mechanics of Materials. Singapore: Springer, 2019: p. 1981–2012.
178. Gonabadi, H., A. Yadav, and S. Bull, Mechanical characterisation of polymeric materials using nanoindentation, in Contact Problems for Soft, Biological and Bioinspired Materials. 2022, Springer. p. 139-180
179. Vranjes-Wessely S, et al. High-speed nanoindentation mapping of organic matter-rich rocks: a critical evaluation by correlative imaging and machine learning data analysis. Int J Coal Geol. 2021;247: 103847.

180. Abedi S, et al. Nanochemo-mechanical signature of organic-rich shales: a coupled indentation–EDX analysis. Acta Geotech. 2016;11:559–72.
181. Yang J, et al. Nanoscale geochemical and geomechanical characterization of organic matter in shale. Nat Commun. 2017;8(1):2179.
182. Eliyahu M, et al. Mechanical properties of organic matter in shales mapped at the nanometer scale. Mar Pet Geol. 2015;59:294–304.
183. Emmanuel S, et al. Impact of thermal maturation on nano-scale elastic properties of organic matter in shales. Mar Pet Geol. 2016;70:175–84.
184. Mehdikhani M, et al. Combining digital image correlation with X-ray computed tomography for characterization of fiber orientation in unidirectional composites. Compos A Appl Sci Manuf. 2021;142: 106234.
185. Holmes J, et al. Digital image and volume correlation with X-ray micro-computed tomography for deformation and damage characterisation of woven fibre-reinforced composites. Compos Struct. 2022;279: 114775.
186. Palanca M, Tozzi G, Cristofolini L. The use of digital image correlation in the biomechanical area: a review. Int Biomech. 2016;3(1):1–21.
187. Blikharskyy Y, et al. Review of development and application of digital image correlation method for study of stress–strain state of RC structures. Appl Sci. 2022;12(19):10157.
188. Pan B, Wang B. Some recent advances in digital volume correlation. Opt Lasers Eng. 2020;135: 106189.
189. Buljac A, et al. Digital volume correlation: review of progress and challenges. Exp Mech. 2018;58:661–708.
190. Dall'Ara E, Tozzi G. Digital volume correlation for the characterization of musculoskeletal tissues: current challenges and future developments. Front Bioeng Biotechnol. 2022;10:1010056.
191. Mylo MD, Poppinga S. Digital image correlation techniques for motion analysis and biomechanical characterization of plants. Front Plant Sci. 2024;14:1335445.
192. Pan B. Digital image correlation for surface deformation measurement: historical developments, recent advances and future goals. Meas Sci Technol. 2018;29(8): 082001.
193. de Pablo JJ, et al. New frontiers for the materials genome initiative. npj Comput Mat. 2019;5(1):41.
194. Mucha, W., et al. 2023. New operational load monitoring approach using digital image correlation and image classification networks. in Journal of Physics: Conference Series. IOP Publishing.